FPI-2068: A novel anti-EGFR/cMET, alpha-particle emitting, radioimmunoconjugate for cancer therapy.

Sadaf Aghevlian[1], Sean Collens[1], Julie Metcalf[1], Natalie Grinshtein[1], John Forbes[1], Frank Comer[2], Darshan Dalal[2], Puja Sapra[2], Eric Burak[1]

[1]Fusion Pharmaceuticals Inc., 270 Longwood Rd. S., Hamilton, ON, Canada L8P 0A6; [2]Astra-Zeneca, Gaithersburg, Maryland, USA.

AACR Poster # **A146**

Abstract (#34683)

Introduction: FPI-2068, a targeted alpha therapeutic (TAT), consists of a humanized EGFR and cMET targeting bispecific antibody (FPI-2053) radiolabeled with actinium-225 [^{225}Ac]. FPI-2068 leverages the EGFR/cMET co-expression in cancer (high vs. low in normal tissues) and internalizing nature of the receptors to deliver radionuclides into tumor cells. The primary tumoricidal mechanism of FPI-2068 is double-strand DNA breaks (DSB) induced by alpha radiation, which leads to cell death.
Methods: FPI-2068 consists of FPI-2053 conjugated with a DOTA-chelate and radiolabeled with [^{225}Ac]. FPI-2071 is the lutetium-177 analogue. The binding and internalization of FPI-2071 was studied *in vitro* using cancer cell lines (HT29 colorectal and H292, H441, H1975, HCC827 lung cancers). *In vivo* studies were performed in corresponding xenograft models. For biodistribution studies FPI-2071 was injected intravenously into mice and tumor/organ radioactivity was quantified *ex vivo* at selected timepoints. For therapeutic studies, a single dose of FPI-2068 was administered to groups of mice over a range from 92.5 to 740 kBq/kg. Excised HT29 and H441 tumors from FPI-2068 treated mice were analyzed by immunoblotting to detect activation of DDR and cell death pathways.
Results: FPI-2071 demonstrated *in vitro* binding to all cell lines tested, followed by internalization and retention of the radioisotope into target cells. The biodistribution profile of FPI-2071 showed low normal organ uptake in all xenograft models tested, while tumor uptake varied. The peak tumor uptake in each model was: H292 (~73 %ID/g), H441 (~38 %ID/g), HT29 (~30 %ID/g), HCC827 (~25 %ID/g) and H1975 (~20 %ID/g). Delivery of FPI-2068 to target xenografts resulted in anti-tumor efficacy; treatment was well-tolerated by animals. Sustained tumor regression (>28 days) was generally observed at doses of 370 kBq/kg and 740 kBq/kg across models. Lower doses were tumor growth suppressive. FPI-2068 treatment resulted in a dose-dependent increase in pATM and pRad50 expression indicating activation of DDR pathways in HT29 and H441 xenografts. Formation of DSB (pH2AX) and the induction of apoptosis (cleaved caspase 3) was also observed, consistent with the proposed primary mechanism of action.
Conclusions: FPI-2068 demonstrated its anti-tumor efficacy in colorectal and lung tumor xenograft mouse models. Single-dose administration of FPI-2068 led to prolonged tumor regression. FPI-2068 caused activation of the DDR pathway as well as apoptosis, suggesting an inability of the cellular machinery to repair the DNA damage induced by the alpha radiation. These data support initiation of clinical trials in patients with solid tumors.

Background: EGFR-cMET target and characteristics of FPI-2068 TAT

EGFR-cMET

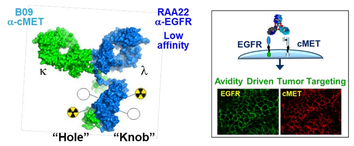

Bispecific rationale

- EGFR & cMET are oncogenic drivers, clear disease link
- Co-expressed & co-upregulated in many solid tumors
- EGFR and cMET mutations and overexpression are key resistance mechanisms to multiple targeted therapies

MOA and differentiation

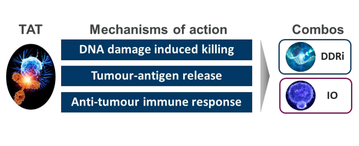

Differentiation

- EGFR affinity reduced to mitigate normal tissue toxicity
- α-emitters: High energy + short range = highly potent
- Primary (DS DNA damage) and secondary (immune response) MOAs provide rationale for combo treatments

Tumor type	EGFR & cMET co-expression >1% TC*	>50% TC*
HNSCC (n=86)	77%	38%
EGFR wtNSCLC (n=210)	94%	48%
CRC (n=150)	94%	61%
Gastric (n=78)	83%	35%
RCC (n=53)	72%	28%
PDAC	88% positive/ 31% highly positive in >50% TC (different methodology used)	

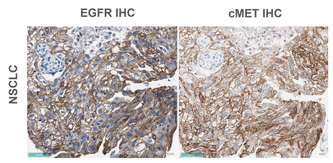

%TC proportion of tumor cells with membrane staining at any intensity level above background using quantitative continuous scoring method (QCS)

High affinity binding with strong cellular internalization and retention *in vitro*; Sustained tumor uptake *in vivo* (Examples)

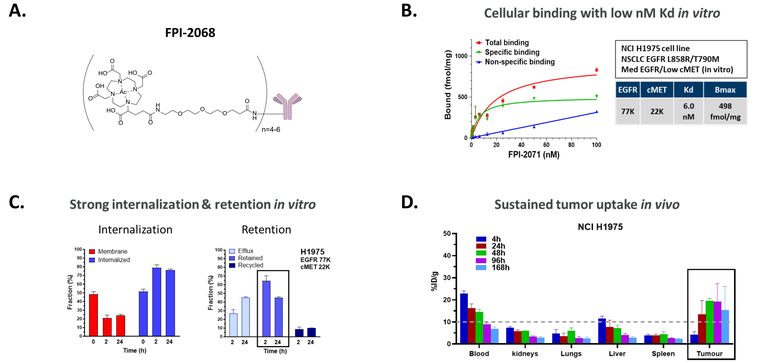

Figure 1. (A) Structure of FPI-2068 radioimmunoconjugate containing Actinium-225. **(B)** *In vitro* binding and **(C)** internalization studies performed with H1975 NSCLC cells and FPI-2071 ([^{177}Lu]-labeled). **(D)** *In vivo* biodistribution (BioD) of FPI-2071 in H1975 xenograft bearing mice.

In vivo efficacy of FPI-2068 in cancer xenograft models (CDX)

HT29 (CRC)

- Durable regression was observed @ 740 kBq/kg

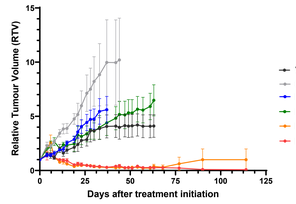

Receptor number: EGFR (52K) > cMET (17K)
Binding data: Kd = 5.7 ± 2.3 nM; Bmax = 2151 ± 237 fmol/mg
Retention @ 24h: **49.8 ± 4.9 %**
Maximal tumor uptake (BioD): 30 ± **4.0** %ID/g @ 96h

H441 (NSCLC)

- Durable regression was observed @ ≥ 370 kBq/kg

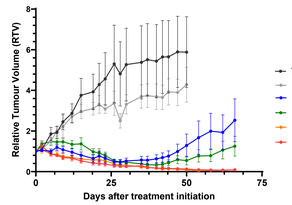

Receptor number: cMET (100K) > EGFR (13K)
Binding data: Kd = 15.4 ± 5.6 nM; Bmax = 1195 ± 153 fmol/mg
Retention @ 24h: **59.4 ± 1.8 %**
Maximal tumor uptake (BioD): 38 ± **11** %ID/g @ 96h

H1975 (NSCLC)

- Durable regression was observed @ ≥ 370 kBq/kg

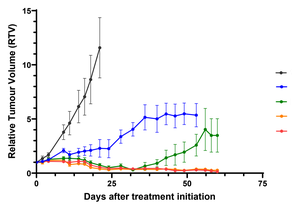

Receptor number: EGFR (77K) > cMET (22K)
Binding data: Kd = 6.0 ± 1.7 nM; Bmax = 499 ± 43 fmol/mg
Retention @ 24h: **45.1 ± 1.6 %**
Maximal tumor uptake (BioD): 19 ± **8.0** %ID/g @ 96h

In vivo efficacy of FPI-2068 in cancer xenograft models (cont'd)

H292 (NSCLC)

- Growth suppression was observed @ ≥ 370 kBq/kg

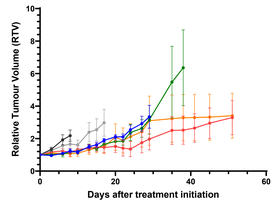

Receptor number: EGFR (418K) > cMET (36K)
Binding data: Kd = 61.6 ± 22.9 nM; Bmax = 4611 ± 884 fmol/mg
Retention @ 24h: **32.0 ± 5.2 %**
Maximal tumor uptake (BioD): 73 ± **7.0** %ID/g @ 96h

Figure 2. Female Balb/c nude mice bearing various human cancer xenografts (n=5 / group) were given single intravenous doses of FPI-2068 (92.5 – 740 kBq/kg) with vehicle and cold antibody control doses. Tumor growth was monitored via caliper measurements. In all cases FPI-2068 treatment was well tolerated with no weight loss or indication of toxicity. The box accompanying each efficacy study summarizes *in vitro* and *in vivo* data for each model. Receptor numbers were determined by flow cytometry.

FPI-2068 causes DSB formation in treated HT29 xenografts while activating DDR response and apoptosis

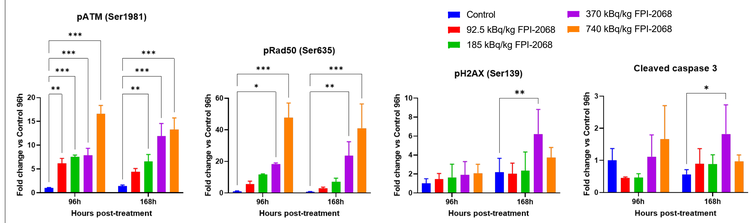

Figure 3. Female Balb/c nude mice bearing HT29 CRC xenografts (n=6 / group) were given single intravenous doses of FPI-2068 (92.5 – 740 kBq/kg) or vehicle control. At selected timepoints, tumors were excised and analyzed for DSB (pH2AX) and DDR markers (pATM, pRAD50) by immunoblotting. Cleaved caspase 3 (apoptosis), and cleaved gasdermin D (pyroptosis) were also analyzed. Gasdermin D was not detected in any samples. Analogous results were obtained using the H441 NSCLC xenograft model (data not shown). Statistical analysis by two-way ANOVA: *P<0.05, **P<0.01,***P<0.001.

Summary

- Preclinical pharmacological assessment of FPI-2068 demonstrated that the radioimmunoconjugate is capable of binding to lung and colorectal cancer cell lines expressing EGFR and cMET receptors and deliver radionuclides inside the cells
- The biodistribution profile of the radioimmunoconjugate showed low normal organ uptake and strong tumor uptake in all xenograft models tested
- Delivery of alpha particles into target cells by FPI-2068 resulted in anti-tumour efficacy in lung and colorectal cancer xenograft bearing mouse models
  - Single doses of FPI-2068 resulted in prolonged tumour regression (>28 days) in most tumour models tested
- FPI-2068 caused treatment induced formation of DSB, which constitute its primary mechanism of action leading to concomitant activation of DDR pathway proteins and apoptosis markers
- Simultaneous targeting of both EGFR and cMET using a bispecific antibody to drive internalization of actinium preferentially into tumor cells co-expressing both targets, while minimizing radiation injury to normal tissue, represents a rational cancer therapeutic paradigm and supports advancement of FPI-2068 into the clinic